

# Using Natural Abundance Radiocarbon To Trace the Flux of Petrocarbon to the Seafloor Following the Deepwater Horizon Oil Spill

Jeffrey Chanton,<sup>\*,†</sup> Tingting Zhao,<sup>‡</sup> Brad E. Rosenheim,<sup>§</sup> Samantha Joye,<sup>||</sup> Samantha Bosman,<sup>†</sup> Charlotte Brunner,<sup>⊥</sup> Kevin M. Yeager,<sup>⊥,#</sup> Arne R. Diercks,<sup>▽</sup> and David Hollander<sup>§</sup>

<sup>†</sup>Department of Earth, Ocean and Atmospheric Science, Florida State University, Tallahassee, Florida 32306-4320, United States

<sup>‡</sup>Department of Geography, Florida State University, Tallahassee, Florida 32306, United States

<sup>§</sup>College of Marine Science, University of South Florida, 140 Seventh Avenue South, St. Petersburg, Florida 33701, United States

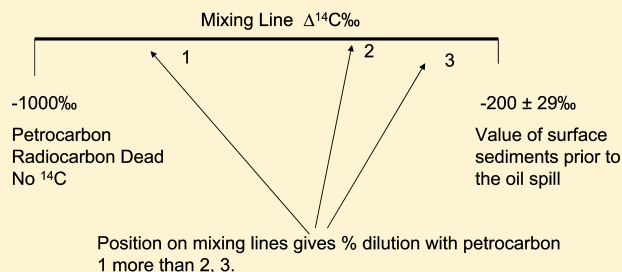
<sup>||</sup>Department of Marine Sciences, University of Georgia, Athens, Georgia 30602, United States

<sup>⊥</sup>Department of Marine Science, University of Southern Mississippi, John C. Stennis Space Center, Mississippi 39529, United States

<sup>#</sup>Department of Earth and Environmental Sciences, University of Kentucky, Lexington, Kentucky 40506, United States

<sup>▽</sup>UM Field Station, University of Southern Mississippi, Abbeville, Mississippi 38601, United States

**ABSTRACT:** In 2010, the Deepwater Horizon accident released  $4.6\text{--}6.0 \times 10^{11}$  grams or 4.1 to 4.6 million barrels of fossil petroleum derived carbon (petrocarbon) as oil into the Gulf of Mexico. Natural abundance radiocarbon measurements on surface sediment organic matter in a  $2.4 \times 10^{10}$  m<sup>2</sup> deep-water region surrounding the spill site indicate the deposition of a fossil-carbon containing layer that included 1.6 to  $2.6 \times 10^{10}$  grams of oil-derived carbon. This quantity represents between 0.5 to 9.1% of the released petrocarbon, with a best estimate of 3.0–4.9%. These values may be lower limit estimates of the fraction of the oil that was deposited on the seafloor because they focus on a limited mostly deep-water area of the Gulf, include a conservative estimate of thickness of the depositional layer, and use an average background or prespill radiocarbon value for sedimentary organic carbon that produces a conservative value. A similar approach using hopane tracer estimated that 4–31% of 2 million barrels of oil that stayed in the deep sea settled on the bottom. Converting that to a percentage of the total oil that entered into the environment (to which we normalized our estimate) converts this range to 1.8 to 14.4%. Although extrapolated over a larger area, our independent estimate produced similar values.



## INTRODUCTION

In 2010 the Deepwater Horizon (DwH) hydrocarbon discharge occurred between April 20 to July 15, 2010, releasing between 50 000 and 70 000 barrels per day, or some 5 million barrels of oil.<sup>2,3</sup> Of this total, 4.1 to 4.6 million barrels were estimated to enter the environment, the difference being the quantity that was captured by on-site containment systems.<sup>2</sup> Once in the environment the hydrocarbons could be transformed by oxidation, consumed by a variety of microbes and likely converted to biomass, burned, or altered in other ways.<sup>4–9</sup> We define this altered and unaltered petroleum-based product as petrocarbon. Because all of it is likely no longer amenable to gas chromatographic separation and analysis,<sup>4,10</sup> the best way to identify it is with a conservative tracer,<sup>1</sup> or isotopically, specifically with radiocarbon.<sup>10–12</sup>

The oil budget calculator group<sup>13</sup> estimated that 16–17% of the total amount of oil was recovered at the well head, 12–13% was naturally dispersed into the water column, 20–25% evaporated or dissolved, 10–20% was chemically dispersed into the water column, 5–6% was burned, 2–4% was skimmed,

and 11–30% was unaccounted for or listed as “other.” Part of this category may include oil deposited to the seafloor.<sup>1,13–16</sup> There are a number of possible mechanisms for such a transfer. First, sedimentation could have resulted from the interaction of petroleum-derived compounds with the high concentrations of marine snow and suspended particulate matter that occurred in the water column and on the surface of the Gulf of Mexico during the time of the oil spill.<sup>14–16</sup> This process was named at a conference as the “Mossfa” (Marine Oil Snow Sedimentation and Flocculent Accumulation) process.<sup>17</sup> Mucous webs were produced in association with oil degradation in the Gulf surface waters and oily particulate matter coagulated with phytoplankton and particulate organic matter.<sup>14–16</sup> These aggregations may have transferred significant quantities of DwH hydrocarbons via rapid sedimentation from the surface to the deep seafloor.<sup>14–16</sup>

**Received:** September 22, 2014

**Revised:** December 6, 2014

**Accepted:** December 12, 2014

This process appeared to be more effective with weathered oil than it was with fresh oil<sup>14</sup> possibly due to the increased polarity of weathered oil caused by the addition of oxygen containing functional groups.<sup>4</sup> Second, in addition to particulate organics, the oil likely interacted with sediment mineral particles in the water column, “OMAs” (Oil Mineral Aggregations or suspended particle aggregations<sup>18–20</sup>). This could have happened as particles passed through surface oil<sup>21</sup> or as particles fell through the deep plume.<sup>1,22–24</sup> A third mechanism for the transfer of petrocarbon to the seafloor was via burning. This mechanism likely consumed 5–6% of the oil,<sup>13</sup> and allowed black carbon and ash to fall to the seafloor. Fourth, zooplankton can transport oil to the sediment in their fecal pellets following ingestion.<sup>19</sup> Fifth, petroleum compounds that spread in a plume to the southwest of the well at depths of 1000 to 1300 m<sup>1,22–24</sup> and that included both dissolved hydrocarbons and small hydrocarbon-rich particles<sup>1</sup> were a likely source of petrocarbon to the seafloor. Microbial cell density was significantly higher than background in this plume,<sup>5</sup> and the plume was dominated by a succession of bacteria, including *Oceanospirillales* and *Colwellia*.<sup>7,8</sup> *Colwellia*, indigenous to the deep Gulf of Mexico, were shown in culture to produce floc consisting of oil, carbohydrates and biomass when incubated with MC-252 oil.<sup>25</sup> *Colwellia* was also abundant in the surface sediments in the area.<sup>26</sup> *Colwellia* and other plume microbes were able to consume a wide range of hydrocarbons including ethane, propane and benzene.<sup>6,7</sup> Valentine et al.<sup>1</sup> suggested that these microbial blooms consumed hydrocarbons, converted a portion of them into biomass, and in addition acted as a flocculate to capture the suspended hydrocarbon-rich particles which led to the deposition and accumulation of microbial biomass, biofilm, and oil-rich particles on the seafloor.<sup>1</sup>

During scientific sampling trips to the Gulf during and after the spill, multiple reports of a rapid sedimentation event suggested that quantities of oil were deposited on the Gulf seafloor.<sup>16</sup> Oil residue on the seafloor could have significant environmental consequences for benthic foodwebs and fauna,<sup>27,28</sup> where it could reside for extended periods of time due to cold temperatures, lack of photochemical alteration and low oxygen if buried. If present in sufficient concentrations, then the oil could inhibit infaunal mixing and remain on the seafloor for longer periods of time. Constraining the amount of DWH derived oil on the seafloor is thus essential.

The objective of this study was to estimate and constrain the amount of oil deposited to the Gulf of Mexico seafloor during the DWH incident using the “inverse” isotopic approach.<sup>10–12</sup> This approach is not sensitive to chemical changes in the oil during the depositional processes described above.<sup>10</sup> We measured the natural abundance radiocarbon (<sup>14</sup>C) content of bulk surface sedimentary organic matter following the spill.<sup>12</sup> Radiocarbon is produced in the atmosphere and has a half-life of 5730 years. Petroleum-derived carbon (petrocarbon) is “fossil,” and being much older than 10 half-lives, its radiocarbon content is nil; it is <sup>14</sup>C dead. Sediments also contain some modern carbon, which is derived from organic material recently fixed from photosynthesis at the surface. This modern carbon contains radiocarbon, which is supplied from the atmosphere. Sedimentary organic material is generally older than current modern values because of the processes of infaunal mixing whereby older sediment layers with depleted radiocarbon content are mixed upward by organisms living in the sediment. The effect of infaunal mixing is minimized in areas where the sediment accumulations rates are high. In addition, in the area of the oil spill, particulate organic carbon (POC) is also supplied by riverine POC derived from a variety of

terrigenous sources and generally has a <sup>14</sup>C content that is depleted relative to modern organic material production.

Our approach rests upon the assumption that prior to the oil spill, sediments were deposited in the Gulf with a more modern <sup>14</sup>C signature than during the event. Before the spill, sources of organic matter to the seafloor included recent photosynthetic production at the sea-surface, sediments and POC from the Mississippi and Atchafalaya Rivers, organic materials from natural seeps, and material from upslope that was advected downward. In 2010 and 2011, superimposed upon this natural background sediment was an overlying layer of sediment containing fossil petrocarbon derived from the DWH spill.

An isotopic approach offers the ability to estimate fresh, weathered, and burned oil content because it does not rely on specific petro-carbon compounds, many of which have been altered following their release.<sup>4,29</sup> Such transformations include reactions driven by surface photochemistry, microbial processes, evaporation, and burning. Indeed, the results of White et al.<sup>10</sup> indicated that discrepancy between a radioisotope mass balance and identification of petroleum hydrocarbons using flame ionization gas chromatography (GC) increased due to the growth of a non GC amenable fraction in the petroleum hydrocarbons in sediments. Using <sup>14</sup>C is a more powerful approach to trace oil content in the sediments than stable isotope composition,  $\delta^{13}\text{C}$ ,<sup>30</sup> because of its greater dynamic range in <sup>14</sup>C composition between oil and its weathering products and possible natural sources of carbon to the sediments.

## ■ METHODS

Sediment samples were collected by multicore samplers using a number of platforms (R.V.s Endeavor, Cape Hatteras, Oceanus, Pelican, and Weatherbird II) from October, 2010 to August, 2012. Cores were sectioned at 1 cm intervals, immediately frozen (−20C), and returned to Florida State University (FSU). Prior to analysis, samples were treated with 10% HCl to remove carbonates, rinsed, freeze-dried, and ground. Samples were then analyzed for percent organic carbon (%C),  $\delta^{13}\text{C}$  and  $\Delta^{14}\text{C}$ . The first two analyses were performed on a Carlo Erba elemental analyzer coupled to a Delta XP Thermo Finnigan isotope ratio mass spectrometer. Results are presented relative to VPDB ( $\delta^{13}\text{C} = (R_{\text{sam}}/R_{\text{std}} - 1) \times 1000$ , where  $R = {}^{13}\text{C}/{}^{12}\text{C}$ ) and the standard is known relative to NBS-19. Sediments for <sup>14</sup>C analysis were combusted at FSU<sup>31</sup> and sent as purified CO<sub>2</sub> (water vapor and noncondensable gases were removed by cryogenic separation on a vacuum line) to the National Ocean Sciences Accelerator Mass Spectrometry Facility (NOSAMS) and to the Lawrence Livermore National Laboratories (LLNL). Samples of CO<sub>2</sub> were prepared as graphite targets at each of these laboratories and analyzed by accelerator mass spectrometry.<sup>32</sup> Values are reported according to the  $\Delta$  notation.<sup>33</sup> The  $\Delta$  notation normalizes the radiocarbon content of a sample to nominal  $\delta^{13}\text{C}$  value (−25‰) and the collection time point. The scale is linear and starts at −1000‰ when a sample has undetectable levels of <sup>14</sup>C, which represents petroleum residue.<sup>10,34,35</sup> Modern carbon, fixed today, has a value of about +35,<sup>36,37</sup> a positive anomaly reflective of additional <sup>14</sup>C in the atmosphere left over from nuclear weapons testing from the late 1940s through early 1960s. The <sup>14</sup>C blanks were generally between 1.2 and 5  $\mu\text{g}$  of C, producing a negligible effect on samples which were over 1200  $\mu\text{g}$  of C. The analysis of 17 replicate sediment samples yields an average analytical reproducibility of  $\pm 6.5\%$ .

Table 1. Radiocarbon Data, 0–1 cm Interval<sup>a</sup>

analysis no.	point	depth (m)	collection date	latitude N°	longitude W°	$\delta^{13}\text{C}\text{‰}$	$\Delta^{14}\text{C}\text{‰}$	%C organic
OS-90632	1	16	11-Oct-10	30.1019	88.7055	-21.2	-105.6	1.6
OS-92593	2	28	11-Oct-10	29.7506	88.5936	-22.9	-267.9	1.8
OS-92677	3	53	11-Oct-10	29.3897	88.6884	-22.8	-249.8	1.4
OS-90557	4	126	13-Oct-10	28.9546	88.9351	-22.6	-192.4	1.9
OS-90291	5	72	12-Oct-10	28.8687	89.6402	-22.7	-148.6	2.0
OS-90564	6	530	12-Oct-10	28.5111	89.8083	-22.5	-201.7	1.5
OS-90552	7	1136	12-Oct-10	28.2397	89.1207	-22.8	-501.0	1.9
OS-90586	8	2360	13-Oct-10	27.9062	88.4500	-21.3	-247.1	1.3
OS-90594	9	1973	15-Oct-10	28.2369	88.3588	-22.5	-162.0	1.6
OS-90412	10	1210	15-Oct-10	28.4379	88.8194	-22.9	-273.2	1.7
OS-90554	11	1207	15-Oct-10	28.7386	88.5565	-21.3	-168.5	2.0
OS-90352	12	1560	16-Oct-10	28.7231	88.4096	-23.1	-432.6	2.7
OS-90547	13	1595	17-Oct-10	28.6373	88.5188	-23.1	-445.2	2.3
OS-90560	14	1570	16-Oct-10	28.7389	88.3403	-21.3	-188.9	1.6
OS-90563	15	2010	19-Oct-10	28.6265	88.2086	-21.2	-107.1	2.1
OS-92594	16	1760	19-Oct-10	28.7566	88.1599	-21.2	-188.6	2.1
OS-90555	17	2180	19-Oct-10	28.7160	87.9014	-21.0	-176.7	1.7
OS-90625	18	2370	18-Oct-10	28.6750	87.6542	-20.8	-170.3	1.5
OS-90415	19	1418	17-Oct-10	28.7706	88.3812	-22.0	-291.1	1.9
OS-90551	20	1160	20-Oct-10	28.9267	88.3263	-21.5	-170.5	2.4
OS-92663	21	1496	5-Sep-10	28.7880	88.1670	-20.6	-198.0	1.4
OS-92667	22	887	7-Sep-10	28.8512	88.4925	-21.2	-323.6	1.6
OS-92585	23	200	9-Sep-10	29.0020	88.8003	-21.5	-146.9	2.2
OS-92586	24	1621	12-Sep-10	28.7075	88.3620	-20.6	-332.1	1.4
OS-92587	25	1920	13-Sep-10	28.5702	88.3235	-20.4	-181.9	1.8
OS-92718	26	1690	14-Sep-10	28.9080	87.9223	-20.5	-169.0	1.6
OS-92588	27	430	15-Sep-10	29.0465	87.5042	-21.1	-110.0	3.0
OS-92595	28	780	15-May-11	29.2050	87.0617	-21.4	-255.5	2.1
OS-96997	29	1300	17-May-11	28.8259	88.2678	-21.1	-254.2	1.5
OS-96999	30	1250	17-May-11	28.8382	88.2505	-21.4	-178.4	1.9
OS-90462	31	1150	17-May-11	28.8905	88.1742	-21.0	-207.9	1.6
OS-90421	32	986	18-May-11	29.1837	87.7478	-21.5	-228.4	2.5
OS-90461	33	614	18-May-11	29.2335	86.7345	-21.2	-216.2	2.5
OS-92597	34	200	18-May-11	29.3182	87.7337	-21.5	-197.2	2.5
OS-92598	35	980	18-May-11	29.1832	87.7487	-21.3	-201.5	2.3
OS-99102	36	1043	1-Dec-10	29.1196	87.2643	-21.3	-202.4	2.4
OS-97908	37	1143	1-Dec-10	28.9767	87.8900	-21.0	-210.2	1.5
OS-9784	38	1520	1-Dec-10	29.1209	87.8655	-20.9	-159.0	2.0
157584	39	1259	24-Oct-11	28.8146	88.4400	-21.6	-191.8	2.5
157585	40	1427	24-Oct-11	28.7430	88.4813	-21.1	-228.1	1.6
157607	41	1398	25-Oct-11	28.7688	88.4315	-21.2	-219.6	1.7
157606	42	1636	26-Oct-11	28.6897	88.3765	-20.9	-230.1	1.5
157605	43	1727	26-Oct-11	28.6390	88.3507	-20.7	-234.7	1.3
157604	44	1752	28-Oct-11	28.7108	88.2408	-20.7	-214.1	1.4
157603	45	1410	24-Oct-11	28.6852	88.5527	-22.0	-315.2	2.0
157602	46	1714	22-Oct-11	28.5853	88.5117	-21.6	-291.1	1.9
157601	47	1863	26-Oct-11	28.5942	88.3162	-17.9	-137.0	2.2
157600	48	1349	22-Oct-11	28.3865	88.8673	-22.3	-239.0	1.5
OS-96309	49	1130	21-Oct-11	28.1013	89.4103	-21.6	-212.2	1.6
OS-96310	50	1220	23-Oct-11	28.6905	88.7355	-21.8	-186.7	1.7
OS-96799	51	1026	23-Oct-11	28.6683	88.8721	-22.2	-207.4	1.2
OS-96804	52	1372	27-Oct-11	28.8615	88.1962	-21.0	-181.1	1.8
OS-102370	53	1795	14-Sep-12	28.3251	88.3877	-21.4	-236.1	1.6
OS-102367	54	1414	11-Sep-12	28.7557	88.3708	-22.2	-268.0	1.8
OS-102500	55	501	22-Apr-12	29.0566	88.3833	-21.5	-144.5	2.6
OS-102456	56	940	30-Jun-12	28.3243	89.4893	-21.5	-194.2	1.8
OS-102457	57	40	2-Jul-12	28.8917	89.8868	-22.0	-206.4	1.6
OS-102458	58	505	30-Jun-12	28.7205	89.0997	-22.1	-176.6	2.0
OS-102459	59	1120	1-Jul-12	28.6527	88.5607	-21.1	-201.9	2.0
OS-102461	60	990	1-Jul-12	28.6607	88.9058	-22.1	-228.8	1.4
OS-102460	61	510	30-Jun-12	28.5292	89.8007	-21.8	-190.2	1.8

Table 1. continued

analysis no.	point	depth (m)	collection date	latitude N°	longitude W°	$\delta^{13}\text{C}\text{‰}$	$\Delta^{14}\text{C}\text{‰}$	%C organic
15793	62	1136	23-Aug-12	28.2209	89.0695	-21.7	-246.7	1.6

<sup>a</sup>OS signifies a NOSAMS identifier, otherwise LLNL CAMS # is signified.

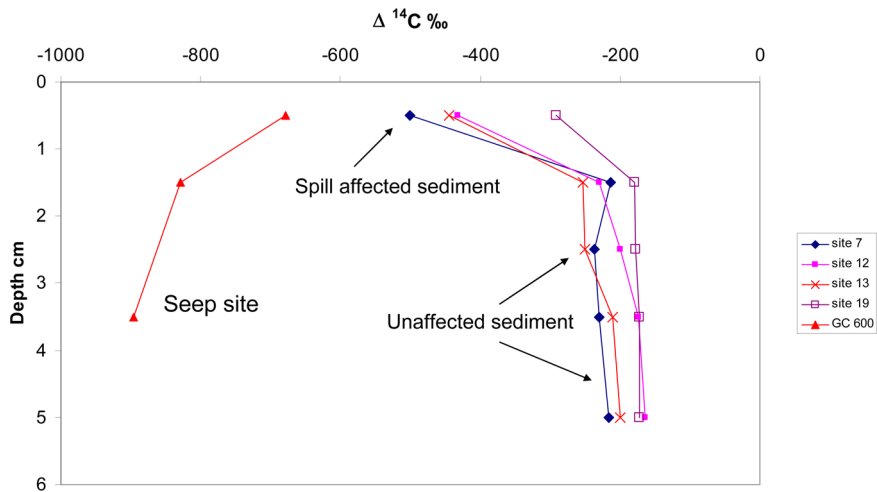


Figure 1. Radiocarbon depth profiles (cm) at selected sites. Site GC-600 is a site known to be naturally affected by oil seepage. The other four sites are interpreted to have a layer of sediments containing fossil carbon from the oil spill overlying background sediment.

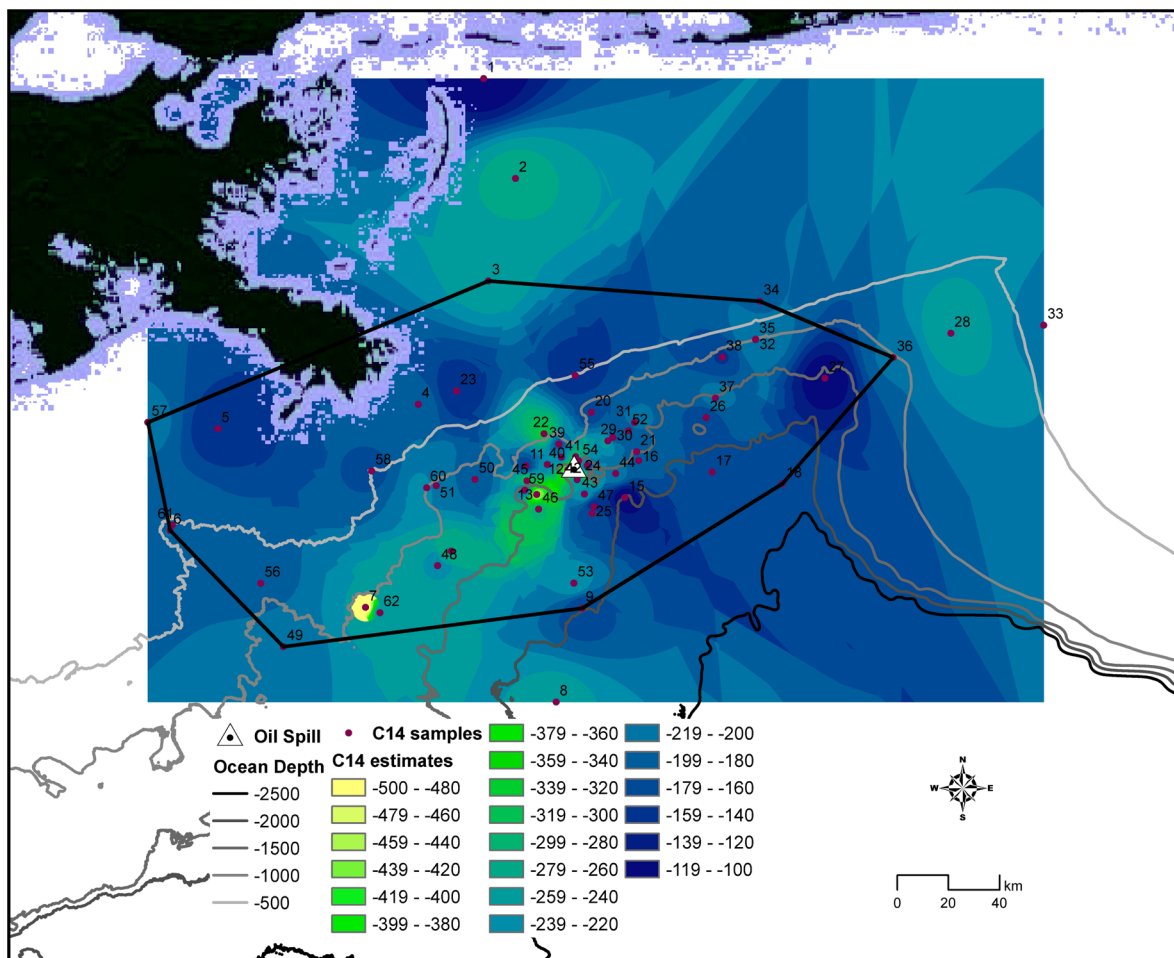


Figure 2. Map of radiocarbon data of seafloor sediments. Each point represents a core sample and the analysis of the surface interval (0–1 cm). Data were contoured with the Inverse Distance Weighting (IDW) method, and within the black polygon, the surface area of each 20‰ interval calculated for the seafloor. This area included 58 of the 62 surface sediments samples that were analyzed.

## RESULTS AND DISCUSSION

Sediment radiocarbon values varied from  $\Delta^{14}\text{C} = -106$  to  $-501\text{‰}$ ,  $\delta^{13}\text{C} = -22.9$  to  $-17.9\text{‰}$ , and % organic carbon = 1.3 to 3.0% in the 0–1 cm interval ( $n = 62$ , Table 1). For surface samples the mean value for  $\Delta^{14}\text{C}$  is  $-219.6 \pm 73.7$ , which is  $^{14}\text{C}$  enriched relative to sediments collected further west of ours and prior to the oil spill at  $-308.6 \pm 84.3$ .<sup>30,38–41</sup> There is a significant trend of radiocarbon depletion from east to west ( $p = 0.0003$ ). Consistent with this finding, Rosenheim et al.<sup>42</sup> reported significant differences in POC age, with the more western Atchafalaya River values depleted in  $\Delta^{14}\text{C}$  by 70% relative to the more eastern Mississippi River POC. The mean value for sediment organic matter  $\delta^{13}\text{C}$  is  $-21.5 \pm 0.8\text{‰}$  which is identical to the mean value for the Gulf reported of  $-21.4 \pm 1.9\text{‰}$  by Rosenheim et al.<sup>30</sup> There were no significant trends with water depth for our  $^{13}\text{C}$  or  $^{14}\text{C}$  data ( $p = 0.37$ ). Our 0–1 cm radiocarbon values are  $^{14}\text{C}$  depleted relative to the 0–1 cm values of the continental slope of the Mid-Atlantic Bight (average,  $-123 \pm 48\text{‰}$ ,  $n = 11$ ,<sup>43</sup>) over a depth range of 415 to 1200 m. Similar to the case here, those authors observed no relationship between  $^{14}\text{C}$  content and water depth in the region they studied.

POC associated with the outflow from the Mississippi River has been reported to range from  $\Delta^{14}\text{C} -86$  to  $-223\text{‰}$  and  $\delta^{13}\text{C} -23.3$  to  $-26.0\text{‰}$ .<sup>44</sup> Rosenheim et al.<sup>42</sup> report bulk Mississippi River POC during a high discharge event in 2008 at  $\Delta^{14}\text{C}$  of  $-226 \pm 7\text{‰}$  (age 2010  $\pm$  67 yrs before present), and during a lower discharge year in 2009 at  $-107.2 \pm 40\text{‰}$  (age 860  $\pm$  350 yrs before present). Atchafalaya River POC during the lower discharge year 2009 had a  $\Delta^{14}\text{C}$  of  $-175 \pm 46\text{‰}$  (age 1500  $\pm$  440 yrs). These two sources of  $^{14}\text{C}$ -depleted organic material obviously affect the northern Gulf of Mexico sediments more than the Mid-Atlantic Bight is affected by riverine POC. To estimate prespill  $^{14}\text{C}$  content of these sediments, we will use the nearly constant values observed below the top 1 cm of sediment (Figure 1). In the northern Gulf of Mexico, input of POC from the Mississippi and Atchafalaya as well as nutrients that feed primary production in the region cause relatively high sediment accumulation rates. Ranges of mm/y to cm/y are not uncommon, thereby both minimizing the age of infaunally mixed old carbon in the sediment surface and outcompeting the depletion of  $^{14}\text{C}$  in the sediments with time. The surface (0–1) cm interval was more depleted in  $^{14}\text{C}$  relative to underlying sediments at 4 sites where we made measurements down to 5 cm depth (Figure 1). This pattern is in contrast to those made at GC 600, a known seep site, where values become more depleted with increasing depth. These results indicate the deposition of radiocarbon depleted petrocarbon within the 0–1 cm interval across the study area, consistent with the findings of Valentine et al.<sup>1</sup>

The 62 radiocarbon surface sediment values (Table 1) were used to estimate  $^{14}\text{C}$  values throughout the study area with the Inverse Distance Weighting (IDW) method provided in ESRI's ArcGIS 10.2. IDW is a spatial interpolation technique that assigns a value to a prediction location (i.e., the place where data value needs to be estimated) using the weighted average of values from nearby sample locations. The weight is proportional to the inverse of Euclidian distance between the prediction location and its nearest sample locations. One exception in this approach was necessary due to a very  $^{14}\text{C}$  depleted value at location 7. The vicinity of location 7 was estimated with the same approach applied to an area enclosed by a radius of 5 km, which helped to confine the spreading of extreme values due to a limited number

of samples in this part of the study area. The two interpolations were integrated to create a single map of the estimated  $\Delta^{14}\text{C}$  value in ‰ (Figure 2). Next, within a polygon ( $2.4 \times 10^{10} \text{ m}^2$ ), where the data density was the greatest and which contained or bordered 58 of our 62 measurements, the continuous estimate of  $^{14}\text{C}$  values was binned by 20%  $\Delta^{14}\text{C}$  units per interval for the seafloor portion of the map. The surface area in  $\text{m}^2$  for each  $^{14}\text{C}$  value interval was also calculated within ArcGIS 10.2 (Table 2).

**Table 2. Average Surface Area in  $\text{m}^2$  for Each  $^{14}\text{C}$  Value Interval Calculated within ArcGIS 10.2**

$\Delta^{14}\text{C} \text{‰}$	$\Delta^{14}\text{C} \text{‰}$	area $\text{m}^2$	fraction	
				fossil C
-500	-480	58 044 918		0.362
-480	-460	1 538 801		0.337
-460	-440	3 305 519		0.312
-440	-420	8 919 105		0.287
-420	-400	10 834 027		0.262
-400	-380	14 509 759		0.237
-380	-360	21 935 015		0.212
-360	-340	30 622 284		0.187
-340	-320	62 870 683		0.162
-320	-300	270 117 259		0.137
-300	-280	301 195 071		0.112
-280	-260	507 897 113		0.087
-260	-240	1 937 592 572		0.062
-240	-220	1 833 747 430		0.037
-220	-200	3 374 841 886		0.012
-200	-180	7 999 736 877		0
-180	-160	5 450 779 431		0
-160	-140	1 503 877 982		0
-140	-120	329 711 269		0
-120	-100	149 488 067		0

Average area (column 3) calculated from a succession of neighbor and power terms (3,1; 3,2; 3,3; 4,1; 4,2; 4,3; 5,1; 5,2; 5,3; 6,1; 6,2; and 6,3), area in  $\text{m}^2$  within each 20% contour (column 1 and 2) and fraction of fossil carbon assuming a background value of  $-200\text{‰}$ .

To estimate the uncertainty of this IDW technique, we varied power (from 1 to 3) and search radius of nearest samples (from 3 to 6 nearest neighbors). A larger search radius encompasses more sample locations to estimate the  $^{14}\text{C}$  value for each prediction location, which assumes weaker spatial autocorrelation of  $^{14}\text{C}$  distribution. An increase in power results in a rapid decrease of weights for distant  $^{14}\text{C}$  samples, which assumes the prediction location resembles the closest samples most. To estimate the uncertainty, we made similar calculations for an array of configurations including (neighbor, power) 3,1; 3,2; 3,3; 4,1; 4,2; 4,3; 5,1; 5,2; 5,3; 6,1; 6,2; and 6,3, and calculated the area within each bin in all of these configurations. This approach also provided us with objective estimates of the uncertainties in the areas within the polygons that were based on different parametrizations. We further crosschecked our IDW contouring with the empirical Bayesian kriging (EBK) technique employed by Valentine et al.<sup>1</sup> using ArcGIS 10.2.

The spatial distribution of the surface sediment radiocarbon values indicate that the bulk radiocarbon depleted material on the seafloor trends to the southwest of the well head, similar to the flow of the subsurface plume<sup>22–24,45–48</sup> and seafloor effects.<sup>1,28,49</sup> To obtain a background value for  $^{14}\text{C}$  value for prespill conditions, we assumed that the values of sediments underlying the surface  $^{14}\text{C}$  depleted layer represented prespill conditions

within the area of the polygon and averaged the 12 values below 2 cm in the cores of Figure 1, excepting of course, GC-600. The average of these data was  $-200 \pm 29\%$ , a value one might arrive at to represent prespill background by a conservative visual inspection of Figure 2. The simplicity of this prespill estimate approach is necessitated by the difficulty and cost of measuring  $^{14}\text{C}$  content of all depth increments of all of our cores; however, it represents a good starting point for this type of budgeting exercise. With constraints on the amount of oil deposited on the seafloor provided by the oil budget calculator,<sup>13</sup> and by other approaches,<sup>1</sup> we can determine whether this assumption is warranted. It may be that this estimate is too conservative, as some  $^{14}\text{C}$  values of surface sediment were  $> -200\%$ . Over the  $2.4 \times 10^{10} \text{ m}^2$  study area only  $8.4 \times 10^9 \text{ m}^2$  or 35% of it was represented by  $\Delta^{14}\text{C}$  values of below  $-200\%$ , interpreted by our conceptual model as affected by petro-carbon deposition.

Our next objective was to calculate the fossil carbon within each area that had been added to or superimposed upon the background  $\Delta^{14}\text{C}$  value of  $-200 \pm 29\%$ . To achieve this, we created a two component mass balance, assuming that the surface sediment (0–1 cm) represented a two end-member mixing of fossil carbon with prespill background sediment organic carbon in the area (eq 1). In this simple mixing model,  $x$  is the fraction of fossil carbon, and  $(1 - x)$  is the fraction of sedimentary carbon that is background carbon. In our approach, fossil (petro-carbon) carbon has a value of  $-1000\%$ , while background carbon has a value of  $-200 \pm 29\%$ .

$$\begin{aligned} \text{measured value} * 1 &= x(-1000\%) \\ &+ (1 - x)(-200 \pm 29\%) \end{aligned} \quad (1)$$

Solving for  $x$ , we obtained the fraction of surface carbon within each area (Table 2) that is fossil carbon. We then multiplied this by the mean measured bulk density,  $0.21 \pm 0.04$ , the mean fraction organic carbon,  $1.9 \pm 0.4\%$ , integrated this to 1 cm and multiplied by the area of each contour in Table 2, and for all the contours described above where we varied neighbors and power. We then summed to obtain the grams of fossil carbon deposited on the seafloor within the polygon of Figure 2. This yields a “best estimate” value of  $1.60 \times 10^{10}$  grams of carbon when averaged over all the ways of contouring the data, from neighbors 3–6 and power 1–3. To account for the uncertainty of this value we propagated all uncertainties assuming no correlation between any of them. This yielded a lower limit value of  $0.3 \times 10^{10}$  g of fossil carbon and upper limit of  $2.9 \times 10^{10}$  g fossil carbon within the polygon (Figure 2) averaged over all the variations of neighbors and contour intervals and the range in % carbon, and bulk density in the 0–1 cm interval. The estimate of oil within the polygon of Figure 2 on the seafloor is thus  $1.60 \pm 1.3 \times 10^{10}$  g of carbon. This estimate was produced by IDW contouring. We additionally compared our value by using empirical Bayesian kriging (EBK)<sup>1</sup> in addition to IDW. Use of EBK contouring, following the approach outlined above yielded a result of  $2.6 \pm 1.6 \times 10^{10}$  g of carbon, within the error of our IDW estimate.

Oil released to the Gulf from the Macondo Blowout from April 20 to July 15, 2010 was estimated to be between 597 454 to 838 070 t of carbon or  $6.0$  to  $8.4 \times 10^{11}$  g of carbon.<sup>3</sup> Other estimates vary from 4.1 to 4.6 million barrels of oil<sup>2,3,13,50</sup> These values convert to  $4.6$  to  $5.1 \times 10^{11}$  g of carbon using an oil density of 820 g per liter at 86% carbon.<sup>46</sup> For our analysis, we will use the Joye et al.<sup>3</sup> lower range as our upper limit ( $6.0 \times 10^{11}$  g carbon), and  $4.6 \times 10^{11}$  g carbon as our lower limit. The midpoint of these two estimates is  $5.3 \times 10^{11}$  g carbon.

Calculating from our best IDW estimate of oil on the seafloor to the midpoint estimate of oil spilled ( $1.6 \times 10^{10}$ )/( $5.3 \times 10^{11}$ ) we find that 3.0% of the oil released by the spill is on the seafloor within our polygon. Our lower limit estimate is  $0.3 \times 10^{10}$  g/ $6.0 \times 10^{11}$  g = 0.5%, while our upper limit is  $2.9 \times 10^{10}$  g/ $4.6 \times 10^{11}$  g = 6.3%. Using our EBK-derived values ( $2.6 \times 10^{10}$ )/( $5.3 \times 10^{11}$ ) yields 4.9% of the oil released by the spill and ranges from 1.7 to 9.1%. Combining these two approaches yields 3.0–4.9% as our best estimate of the amount of the oil that was deposited on the seafloor, with a range of from 0.5 to 9.1%.

Jernelov and Linden<sup>51</sup> speculated that 25% of the 475 000 t of oil released from the 1979 Ixtoc spill went to the seafloor. These authors noted that the Ixtoc oil became denser as fractions of it evaporated and dissolved, and postulated that the residual oil sank to the seafloor. However, there was no confirmation of the estimate. This spill occurred in much shallower water (only 50 m), and it may be that the water column was more sediment laden which could also have caused greater transport of oil to the seafloor. Ajijolaiya et al.<sup>18</sup> demonstrated that oil mineral interactions are clearly dependent upon the quantity of sediment in the water column and describe threshold concentrations at which the process of oil aggregation initiates. They point out that because oil mineral aggregation is critically dependent upon threshold concentrations of minerals in the water column there are important implications regarding the proximity of oil spills relative to river mouths and other coastal sediment sources and areas of high productivity where transport of petrocarbon to the seafloor will clearly be greater due to interaction of oil with minerals and suspended particulates. Interaction of oil and suspended particulate matter will increase the density of hydrocarbons, causing more rapid sedimentation.<sup>19</sup> Because oil production is closely associated with deltaic regions, these relationships between particulate matter and oil will be the rule rather than the exception. Other factors of importance include size and dominant mineralogy of the inorganic fraction and of course, interaction with dispersants.<sup>52</sup>

In addition, black carbon, produced from the incomplete combustion of oil at the sea surface during the spill could have promoted rapid sediment deposition. Black carbon is very surface active<sup>53</sup> and its deposition in marine systems leads to an increase in the concentration of suspended particles, stimulation of aggregation of particles, absorption of dissolved organic carbon and increases in bacterial abundance.<sup>54</sup> This could also have been important in generating the mucous webs and abundant phytoplankton which interacted with the oil, causing sedimentation as discussed above.<sup>14,15</sup>

As pointed out by Muschenheim and Lee,<sup>19</sup> researchers tend to view processes that remove spilled hydrocarbons from the area that they are interested in as being beneficial. These authors give the example of plankton scientists who see oil-particulate interaction as a benevolent process as it removes oil from the water. However, as they point out, biotic and abiotic hydrocarbon degradation occurs at a faster rate in the water column relative to sediments where these degradation rates are attenuated, particularly for aromatic compounds. Thus, sediments may serve as long-term storage for hydrocarbons for as yet unknown periods of time. With that storage, there is potential for re-exchange with the water column due to either chemical or physical processes that occur in surface sediments including benthic predation, chemical degradation, and infaunal mixing.<sup>27</sup>

Our best estimate is that 3.0–4.9% of the oil spilled in the Deepwater Horizon event from April 20 to July 15, 2010 was deposited in a  $2.4 \times 10^{10} \text{ m}^2$  region surrounding the wellhead.

Uncertainty in this estimate, given the assumptions made, ranges from 0.5 to 9.1% of the total oil spilled. Our approach has three caveats that result in our estimation producing a conservative lower limit of deposition. First, our focus is over a limited area of the Gulf surrounding the wellhead. Second, we have only integrated the fossil carbon-rich layer to a depth of 1 cm, while thicker depositions were observed in limited areas.<sup>16</sup> Third, we chose a background value of  $\Delta^{14}\text{C}$  of  $-200 \pm 29\%$  even though more positive surface sediment values were measured in the study area, which leads to a relatively conservative estimate of petrocarbon on the seafloor. However, the oil budget calculator group<sup>13</sup> reported that 11–30% of the oil was unaccounted for or listed as “other.” We hypothesized that a particular component of this “other” category may have been transported to the seafloor by a number of mechanisms. Our estimates are within the bounds of this category, and are similar to the quantity of seafloor oil (1.8 to 14.4% of the total released) determined by Valentine et al.<sup>1</sup> using an independent technique.

## AUTHOR INFORMATION

### Corresponding Author

\*Phone: 850-644-7493; e-mail: jchanton@fsu.edu.

### Notes

The authors declare no competing financial interest.

## ACKNOWLEDGMENTS

We thank the captains and crews of the R.V.s Endeavor, Cape Hatteras, Oceanus, Pelican and Weatherbird II. We thank Katheryn Elder, Sue Handwork, and Ann McNichol at NOSAMS and Tom Guilderson at LLNL for AMS work, and Olivia Mason for microbial consultations. We are appreciative to four anonymous reviewers for helpful suggestions, and to the editor, Dr. P. Alvarez, who handled our submission. This research was funded by grants from BP/The Gulf of Mexico Research Initiative: to the Deep-C research consortium administered by Florida State University, to the consortium “Ecosystem Impacts of Oil and Gas Inputs to the Gulf” (ECOGIG) administered by the University of Mississippi, to the Northern Gulf Institute, administered by Mississippi State University, to the Consortium for the Advanced Research of Transport of Hydrocarbon in the Environment (CARTHE), administered by the University of Miami, and to the Center for Integrated Modeling and Analysis of Gulf Ecosystems, administered by the University of South Florida. This is ECOGIG contribution #305 and the data are available under GRIDCC UDI: R1.x138.078:0024.

## REFERENCES

- (1) Valentine, D. L.; Fisher, G. B.; Bagby, S. C.; Nelson, R. K.; Reddy, C. M.; Sylva, S. P.; Woo, M. A. Fallout plume of submerged oil from Deepwater Horizon. *Proc. Natl. Acad. Sci. U. S. A.* **2014**, DOI: 10.1073/pnas.1414873111.
- (2) McNutt, M. K.; Camilli, R.; Crone, T. J.; Guthrie, G. D.; Hsieh, P. A.; Ryerson, T. B.; Savas, O.; Shaffer, F. Review of flow rate estimates of the Deepwater Horizon oil spill. *Proc. Natl. Acad. Sci. U. S. A.* **2012**, *109*, 20260–20267 DOI: /10.1073/pnas.1112139108.
- (3) Joye, S. B.; MacDonald, I. R.; Leifer, I.; Asper, V. Magnitude and oxidation potential of hydrocarbon gases released from the BP oil well blowout. *Nat. Geosci.* **2011**, *4*, 160–165.
- (4) Aeppli, C.; Carmichael, C. A.; Nelson, R. K.; Lemkau, K. L.; Graham, W. M.; Redmond, M. C.; Valentine, D. L.; Reddy, C. M. Oil weathering after the Deepwater Horizon spill led to formation of oxygenated residues. *Environ. Sci. Technol.* **2012**, *46*, 8799–8807.
- (5) Hazen, T. C.; Dubinsky, E. A.; DeSantis, T. Z.; Andersen, G. L.; Piceno, Y. M.; Singh, N.; Jansson, J. K.; Probst, A.; Borglin, S. E.;

Fortney, J. L.; Stringfellow, W. T.; Bill, M.; Conrad, M. E.; Tom, L. M.; Chavarria, K. L.; Alusi, T.; Lamendella, R.; Spier, C.; Baelum, J.; Auer, M.; Zemla, M. L.; Chakraborty, R.; Sonnenthal, E. L.; D’haeseleer, P.; Ying, H.; Holman, N.; Osman, S.; Lu, Z.; Van Nostrand, J. D.; Deng, Y.; Zhou, J.; Mason, O. U. Deep-sea oil plume enriches indigenous oil-degrading bacteria. *Science* **2010**, *330*, 204–208.

(6) Valentine, D. L.; Kessler, J. D.; Redmond, M. C.; Mendes, S. D.; Heintz, M. B.; Farwell, C.; Hu, L.; Kinnaman, F. S.; Yvon-Lewis, S.; Du, M.; Chan, E. W.; Tigreros, F. G.; Illanueva, C. J. Propane respiration jump-starts microbial response to a deep oil spill. *Science* **2010**, *330*, 208–211.

(7) Redmond, M. C.; Valentine, D. L. Natural gas and temperature structured a microbial community response to the Deepwater Horizon oil spill. *Proc. Natl. Acad. Sci. U. S. A.* **2012**, *109*, 20292–20297.

(8) Dubinsky, E. A.; Conrad, M. E.; Chakraborty, R.; Bill, M.; Borglin, S. E.; Hollibaugh, J. T.; Mason, O. U.; Piceno, Y. M.; Reid, F. C.; Stringfellow, W. T.; Tom, L. M.; Hazen, T. C.; Andersen, G. L. Succession of hydrocarbon-degrading bacteria in the aftermath of the Deepwater Horizon oil spill in the gulf of Mexico. *Environ. Sci. Technol.* **2013**, *47*, 10860–10867.

(9) Mason, O. U.; Hazen, T. C.; Borglin, S.; Chain, P. S. G.; Dubinsky, E. A.; Fortney, J. L.; Han, J.; Holman, H. Y. N.; Hultman, J.; Lamendella, R.; Mackelprang, R.; Malfatti, S.; Tom, L. M.; Tringe, S. G.; Woyke, T.; Zhou, J.; Rubin, E. M.; Jansson, J. K. Metagenome, metatranscriptome and single-cell sequencing reveal microbial response to Deepwater Horizon oil spill. *ISME J.* **2012**, *6*, 1715–1727 DOI: 10.1038/ismej.2012.59.

(10) White, H. K.; Reddy, C. M.; Eglinton, T. I. Radiocarbon-based assessment of fossil fuel derived contaminant associations in sediments. *Environ. Sci. Technol.* **2008**, *42* (15), 5428–5434.

(11) Reddy, C. M.; Pearson, A.; Xu, L.; McNichol, A.; Benner, B. A.; Wise, S. A.; Klouda, G. A.; Currie, L. A.; Eglinton, T. I. Radiocarbon as a tool to apportion the sources of polycyclic aromatic hydrocarbons and black carbon in environmental samples. *Environ. Sci. Technol.* **2002**, *36*, 1774–1782.

(12) White, H. K.; Reddy, C. M.; Eglinton, T. I. Isotopic constraints on the fate of petroleum residues sequestered in salt marsh sediments. *Environ. Sci. Technol.* **2005**, *39* (15), 2545–2551.

(13) Lehr, W.; Bristol, S.; Possolo, A. Federal Interagency Solutions Group, Oil budget calculator science and engineering team. Oil Budget Calculator. Technical document [http://www.restorethegulf.gov/sites/default/files/documents/pdf/OilBudgetCalc\\_Full\\_HQ-Print\\_111110.pdf](http://www.restorethegulf.gov/sites/default/files/documents/pdf/OilBudgetCalc_Full_HQ-Print_111110.pdf), 2010. Last accessed, July 24, 2014.

(14) Passow, U.; Ziervogel, K.; Asper, V.; Diercks, A. Marine snow formation in the aftermath of the Deepwater Horizon oil spill in the Gulf of Mexico. *Environ. Res. Lett.* **2012**, *7*, 035301.

(15) Ziervogel, K.; McKay, L.; Rhodes, B.; Osburn, C. L.; Dickson-Brown, J. Microbial activities and dissolved organic matter dynamics in oil-contaminated surface seawater from the Deepwater Horizon oil spill site. *PLoS One* **2012**, *7* (4), e34816 DOI: 10.1371/journal.pone.0034816.

(16) Joye, S. B.; Teske, A. P.; Kostka, J. E. Microbial dynamics following the Macondo oil well blowout across Gulf of Mexico environments. *BioScience* **2014**, *64*, 766 DOI: 10.1093/biosci/biu121.

(17) Kinner, N. E.; Belden, L.; Kinner, P. Unexpected sink for Deepwater Horizon oil may influence future spill response. *Eos* **2014**, 95.

(18) Ajjajolaiya, L. O.; Hill, P. S.; Khelifa, A.; Islam, R. M.; Lee, K. Laboratory investigation of the effects of mineral size and concentration on the formation of oil–mineral aggregates. *Mar. Pollut. Bull.* **2006**, *52*, 920–927.

(19) Muschenheim, D. K.; Lee, K. Removal of oil from the sea surface through particulate interactions: review and prospectus. *Spill Sci. Technol. Bull.* **2002**, *8*, 9–18.

(20) LeFloch, S.; Guyomarch, J.; Merlin, F. X.; Stoffyn-Egli, P.; Dixon, J.; Lee, K. The influence of salinity on oil–mineral aggregate formation. *Spill Sci. Technol. Bull.* **2002**, *8*, 75–71.

(21) Garcia-Pineda, O.; MacDonald, I.; Hu, C.; Svejksky, J.; Hess, M.; Dukhovskoy, D.; Morey, S. L. Detection of floating oil anomalies

from the Deepwater Horizon oil spill with synthetic aperture radar. *Oceanography (Wash DC)* **2013**, *26*, 124–137.

(22) Spier, C.; Stringfellow, W. T.; Hazen, T. C.; Conrad, M. Distribution of hydrocarbons released during the 2010, MC252 oil spill in deep offshore waters. *Environ. Pollut.* **2013**, *173*, 224–230.

(23) Camilli, R.; Reddy, C. M.; Yoerger, D. R.; Van Mooy, B. A. S.; Jakuba, M. V.; Kinsey, J. C.; McIntyre, C. P.; Sylvia, S. P.; Maloney, J. V. Tracking hydrocarbon plume transport and biodegradation at Deepwater Horizon. *Science* **2010**, *330*, 201–204.

(24) Ryerson, T. B.; Camilli, R.; Kessler, J. D.; Kujawinski, E. B.; Reddy, C. M.; Valentine, D. L.; Atlas, E.; Blake, D. R.; de Gouw, J.; Meinardi, S.; Parrish, D. D.; Peischl, J.; Seewald, J. S.; Warneke, C. Chemical data quantify Deepwater Horizon hydrocarbon flow rate and environmental distribution. *Proc. Natl. Acad. Sci. U. S. A.* **2012**, *109*, 20246–20253.

(25) Bælum, J.; Borglin, S.; Chakraborty, R.; Fortney, J. L.; Lamendella, R.; Mason, O. U. Deep-sea bacteria enriched by oil and dispersant from the Deepwater Horizon spill. *Environ. Microbiol.* **2012**, *14*, 2405–2416.

(26) Mason, O. U.; Scott, N. M.; Gonzalez, A.; Robbins-Pianka, A.; Bælum, J.; Kimbrel, J.; Bouskill, N. J.; Prestat, E.; Borglin, S.; Joyner, D. C.; Fortney, J. L.; Jurelevicius, D. W.; Stringfellow, T.; Alvarez-Cohen, L.; Hazen, T. C.; Knight, R.; Gilbert, J. A.; Jansson, J. K. Metagenomics reveals sediment microbial community response to Deepwater Horizon oil spill. *ISME J.* **2014**, *8*, 1464–1475.

(27) Murawski, S. A.; Hogarth, W. T.; Peebles, E. B.; Barbeiri, L. Prevalence of external skin lesions and polycyclic aromatic hydrocarbon concentrations in Gulf of Mexico fishes, post-Deepwater Horizon. *Trans. Am. Fish. Soc.* **2014**, *143*, 1084–1097 DOI: 10.1080/00028487.2014.911205.

(28) Montagna, P. A.; Baguley, J. G.; Cooksey, C.; Hartwell, I.; Hyde, L. J.; Hyland, J. L.; Kalke, R. D.; Kracker, L. M.; Reuscher, M.; Rhodes, A. C. E. Deep-sea benthic footprint of the Deepwater Horizon blowout. *PLoS One* **2013**, *8*, 10.1371/journal.pone.0070540.

(29) Pendergraft, M. A.; Rosenheim, B. E. Varying relative degradation rates of oil in different forms and environments revealed by ramped pyrolysis. *Environ. Sci. Technol.* **2014**, DOI: 10.1021/es501354c.

(30) Rosenheim, B. E.; Pendergraft, M. A.; Flowers, G. C.; Carney, R.; Sericano, J.; Amer, R. M.; Chanton, J.; Dincer, Z.; Wade, T. Employing extant stable carbon isotope data in Gulf of Mexico sedimentary organic matter for oil spill studies. *Deep-Sea Res.*, in press.

(31) Choi, Y.; Wang, Y. Dynamics of carbon sequestration in a coastal wetland using radiocarbon measurements. *Global Biogeochem. Cycles* **2004**, *18*, GB4016 DOI: 10.1029/2004GB002261.

(32) Vogel, J. S.; Southon, J. R.; Nelson, D. E.; Brown, T. A. Performance of catalytically condensed carbon for use in accelerator mass spectrometry. *Nucl. Instrum. Methods Phys. Res.* **1984**, *B5*, 289–293.

(33) Stuiver, M.; Polach, H. A. Reporting of <sup>14</sup>C Data. *Radiocarbon* **1977**, *19*, 355–363.

(34) McNichol, A. P.; Aluwihare, L. I. The power of radiocarbon in biogeochemical studies of the marine carbon cycle: Insights from studies of dissolved and particulate organic carbon (DOC and POC). *Chem. Rev.* **2007**, *443*–466.

(35) Trumbore, S. E. Radiocarbon and soil carbon dynamics. *Annu. Rev. Earth Planet. Sci.* **2009**, *37*, 47–66.

(36) Graven, H. D.; Guilderson, T. P.; Keeling, R. F. Observations of radiocarbon in CO<sub>2</sub> at LaJolla, California USA 1992–2007, Analysis of a long term trend. *J. Geophys. Res.* **2012**, D02302 DOI: 10.1029/2011JD016533.

(37) Chanton, J. P.; Cherrier, J.; Wilson, R. M.; Sarkodee-Adoo, J.; Bosman, S.; Mickle, A.; Graham, W. M. Radiocarbon indicates that carbon from the Deepwater Horizon spill entered the planktonic food web of the Gulf of Mexico. *Environ. Res. Lett.* **2012**, *7*, 045393 DOI: 10.1088/1748-9326/7/4/045303.

(38) Goñi, M. A.; Ruttnerberg, K. C.; Eglinton, T. I. Source and contribution of terrigenous organic carbon to surface sediments in the Gulf of Mexico. *Nature* **1997**, *389*, 275–278.

(39) Gordon, E. S.; Goñi, M. A. Sources and distribution of terrigenous organic matter delivered by the Atchafalaya River to sediments in the northern Gulf of Mexico. *Geochim. Cosmochim. Acta* **2003**, *67*, 16–26.

(40) Gordon, E. S.; Goñi, M. A. Controls on the distribution and accumulation of terrigenous organic matter in sediments from the Mississippi and Atchafalaya River margin. *Mar. Chem.* **2004**, *92*, 22–31.

(41) Gordon, E. S.; Goni, M. A.; Roberts, Q. N.; Kineke, G. C.; Allison, M. A. Organic matter distribution and accumulation on the inner Louisiana shelf west of the Atchafalaya River. *Cont. Shelf Res.* **2001**, *21*, 1691–1721.

(42) Rosenheim, B. E.; Roe, K. M.; Roberts, B. J.; Allison, M. A.; Kolker, A. S.; Johannesson, K. H. River discharge influences on particulate organic carbon age structure in the Mississippi/Atchafalaya River System. *Global Biogeochem. Cycles* **2013**, *27*, 154–166.

(43) Demaster, D. J.; Thomas, C. J.; Blair, N. E.; Fornes, W. L.; Plaia, G.; Levin, L. Deposition of bomb <sup>14</sup>C in continental slope sediments of the Mid-Atlantic Bight: assessing organic matter sources and burial rates. *Deep-Sea Res. II* **2002**, *49*, 4667–4685.

(44) Laodong Guo, personal communication, 2013.

(45) Kessler, J. D.; Valentine, D. L.; Redmond, M. C.; Du, M.; Chan, E. W.; Mendes, S. D.; Quiroz, E. W.; Villanueva, C. J.; Shusta, S. S.; Werra, L. M.; Yvon-Lewis, S. A.; Weber, T. C. A persistent oxygen anomaly reveals the fate of spilled methane in the deep Gulf of Mexico. *Science* **2011**, *331*, 312–315.

(46) Reddy, C. M.; Arey, J. S.; Seewald, J. S.; Sylva, S. P.; Lemkau, K. L.; Nelson, R. K.; Carmichael, C. A.; McIntyre, C. P.; Fenwick, J.; Ventura, G. T.; Van Mooy, B. A. S.; Camilli, R. Composition and fate of gas and oil released to the water column during the Deepwater Horizon oil spill. *Proc. Natl. Acad. Sci. U. S. A.* **2012**, *109*, 20229–20234 www.pnas.org/cgi/doi/10.1073/pnas.1101242108.

(47) Du, M. R.; Kessler, J. D. Assessment of the spatial and temporal variability of bulk hydrocarbon respiration following the Deepwater Horizon oil spill. *Environ. Sci. Technol.* **2012**, *46*, 10,499–10,507.

(48) Crespo-Medina, M.; Meile, C. D.; Hunter, K. S.; Diercks, A. R.; Asper, V. L.; Orphan, V. J.; Tavormina, P. L.; Nigro, L. M.; Battles, J. J.; Chanton, J. P.; Shiller, A. M.; Joung, D. J.; Amon, R. M. W.; Bracco, A.; Montoya, J. P.; Villareal, T. A.; Wood, A. M.; Joye, S. B. The rise and fall of methanotrophy following a deepwater oil-well blowout. *Nat. Geosci.* **2014**, *7*, 423–427.

(49) White, H. K.; Hsing, P. Y.; Cho, W.; Shank, T. M.; Cordes, E. E.; Quattrini, A. M.; Nelson, R. K.; Camilli, R.; Demopoulos, A. W. J.; German, C. R. Impact of the Deepwater Horizon oil spill on a deep-water coral community in the Gulf of Mexico. *Proc. Natl. Acad. Sci. U. S. A.* **2012**, *109* (50), 20,303–20,308.

(50) Griffiths, S. K. Oil release from Macondo well MC252 following the Deepwater Horizon accident. *Environ. Sci. Technol.* **2012**, *46*, 5616–5622 DOI: org/10.1021/es204569t.

(51) Jernelov, A.; Linden, O.; Ixtoc, I. A case study of the world's largest oil spill. *Ambio* **1981**, *10*, 299–306.

(52) Sorensen, L.; Melbye, A. G.; Booth, A. M. Oil droplet interaction with suspended sediment in the seawater column: Influence of physical parameters and chemical dispersants. *Mar. Pollut. Bull.* **2014**, *78*, 146–152.

(53) Koelmans, A. A.; Jonker, M. T. O.; Cornelissen, G.; Bucheli, T. D.; Van Noort, P. C. M.; Gustafsson, Ö Black carbon: The reverse of its dark side. *Chemosphere* **2006**, *63*, 365–377 DOI: 10.1016/j.chemosphere.2005.08.034.

(54) Mari, X.; Lefèvre, J.; Torrèton, J. P.; Bettarel, Y.; Pringault, O.; Rochelle-Newall, E.; Marchesiello, P.; Menkes, C.; Rodier, M.; Migon, C.; Motegi, C.; Weinbauer, M. G.; Legendre, L. Effects of soot deposition on particle dynamics and microbial processes in marine surface waters. *Global Biogeochem. Cycles* **2014**, 2014GB004878 DOI: 10.1002/2014GB004878.